Electron. Mater. Lett., Vol. 10, No. 6 (2014), pp. 1115-1120
DOI: 10.1007/s13391-014-4128-0

AlGaN/GaN MOSHFET Power Switching Transistor with Embedded Fast Recovery Diode

Jung-Yeon Lee,[1] Bong-Ryeol Park,[1] Hyungtak Kim,[1] Jaehan Kim,[2] and Ho-Young Cha[1,*]

[1]School of Electronic and Electrical Engineering, Hongik University, Seoul 121-791, Korea
[2]KEPCO Research Institute, Daejeon 305-760, Korea

(received date: 18 April 2014 / accepted date: 15 May 2014 / published date: 10 November 2014)

In this study, a novel AlGaN/GaN power-switching device is proposed for use in high-efficiency DC-DC converters. The proposed structure is composed of a normally-off AlGaN/GaN metal-oxide-semiconductor heterojunction field-effect transistor (MOSHFET) and an embedded freewheeling Schottky barrier diode (SBD). The effects of the embedded freewheeling SBD on conversion efficiency were investigated based on circuit simulation of DC-DC synchronous buck converters. The SBD embedment not only reduces the chip size and cost, but also improves the power conversion efficiency at high operation frequencies, due to the reduced off-state power loss.

Keywords: AlGaN/GaN, conversion efficiency, freewheeling diode, metal-oxide-semiconductor heterojunction field-effect transistor, synchronous buck converter

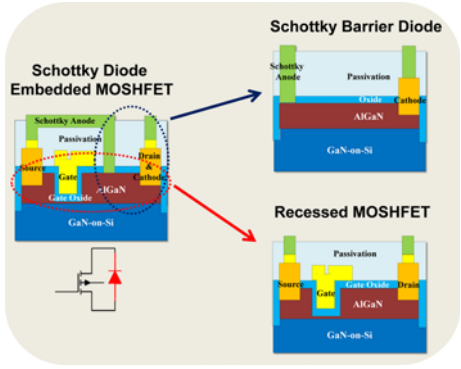

1. INTRODUCTION

AlGaN/GaN heterostructures are a promising candidate for use in high-power and high-efficiency switching applications, owing to their superior material properties, such as their high breakdown field and high electron mobility. In particular, AlGaN/GaN wafers grown on silicon substrates have gained additional attention due to their cost competitiveness with current Si power devices. AlGaN/GaN based prototype devices and power ICs have already demonstrated significantly lower on-resistance values and improved conversion efficiency, in comparison with current state-of-the-art Si counterparts.[1-3] Implementation of normally-off mode operation, which was a critical barrier slowing the advancement of AlGaN/GaN transistor technology, has been resolved using several different approaches, including gate injection transistors, recessed MISFETs, and cascode configuration using Si MOSFET.[4-8]

The DC-DC buck converter is a popular voltage step-down converter consisting of a switching device and a rectifier. A diode is used as a lower side rectifier in basic buck converter topology, whereas it is replaced by a switching transistor in synchronous buck converters in order to improve the conversion efficiency. The higher and lower side switches in a synchronous buck converter must be turned on alternatively, which requires 'dead-time' between switching states to avoid simultaneous ON states. When a Si power MOSFET is used as a lower side switch, a body diode of MOSFET allows the reverse current flow during the dead-time period. As soon as the MOSFET is turned on, the MOSFET takes over the reverse current to minimize the power loss; a body diode typically has a higher on-resistance value than a MOSFET. Therefore, the power loss caused by the body diode during the dead-time period must be carefully taken into account when designing a power converter. This power loss is extremely important when the switching frequency becomes higher. Though AlGaN/GaN based FETs do not have a body diode common to Si power MOSFETs, they exhibit similar function in reverse bias operation; when the magnitude of reverse drain bias is sufficiently increased with a fixed zero gate voltage, the gate bias relative to the drain voltage will exceed the threshold voltage, which in turn allows the electrons from the drain electrode to flow to the source electrode. Accordingly, the source-to-drain voltage drop during reverse conduction mode is always higher than the threshold voltage of AlGaN/GaN FET. That is, the higher the threshold voltage, the

*Corresponding author: hcha@hongik.ac.kr

higher the dead-time power loss. A simple solution to reduce dead-time power loss would be to connect an external freewheeling diode with fast recovery and low turn-on voltage characteristics. However, it is obvious that this solution would increase the overall cost and size of the converter. Morita *et al.* developed a GaN-on-Si FET with an integrated Si Schottky barrier diode (SBD) built in the Si substrate to reduce the reverse turn-on voltage.[9] The drawbacks of this approach would be the complicated fabrication process and the operating temperature range limited by the Si SBD. In this letter, we present a novel AlGaN/GaN FET structure that has an embedded fast recovery freewheeling diode with a low turn-on voltage.

2. EXPERIMENTS AND DISCUSSION

2.1 The Effects of a Freewheeling Diode in a GaN Based DC-DC Synchronous Buck Converter

In addition to the advantage of high power density, the switching speed of GaN based power FETs is significantly faster than that of Si power devices. Therefore, GaN based power ICs can be operated at much higher switching frequencies, which will reduce the size of passive components, and thus reduce the overall size and weight of power ICs. However, it should be noted that the conversion efficiency decreases as the switching frequency increases. It is obvious that the dead-time power loss plays an important role in conversion efficiency at high switching frequency, where the dead-time period is not negligible anymore. In such a case, adding a freewheeling fast recovery diode will minimize the power loss.

In order to investigate the effects of a freewheeling diode in GaN based power converters, DC-DC synchronous buck converters were designed using a commercially available SBD (Model: MBR20100)[10] in conjunction with GaN FETs (Model: EPC2010).[11] The schematic of a 60 V - 10 V down converter consisting of GaN FET only switches is shown in Fig. 1(a). The GaN FETs are driven with a 5 V pulse. The stray inductance caused by wiring FETs is assumed to be 100 pH. In Fig. 1(b), an additional freewheeling SBD is connected to the lower side GaN FET switch for comparison. The SBD used in this simulation has a threshold voltage of 0.43 V. Current-voltage characteristics of the GaN FET alone and the SBD-combined GaN FET are compared in Fig. 2. The gate bias voltages (V_{gs}) for ON- and OFF-states were 5 and 0 V, respectively. Superior characteristics in reverse conduction mode (i.e. third quadrant of the plot) are observed for the SBD-combined FET.

The conversion efficiency was calculated via simulation, measuring steady state input and output power. Load current and switching frequency were varied during the simulation. Conversion efficiency, acting as a function of the switching frequency for the circuits, with and without a freewheeling diode, are shown in Fig. 3, where the simulations were carried out for a constant load current of 2 A with a dead-time period of 10 ns. The efficiency drops as the switching frequency increases. The efficiency improvement using a freewheeling diode becomes noticeable at frequencies higher

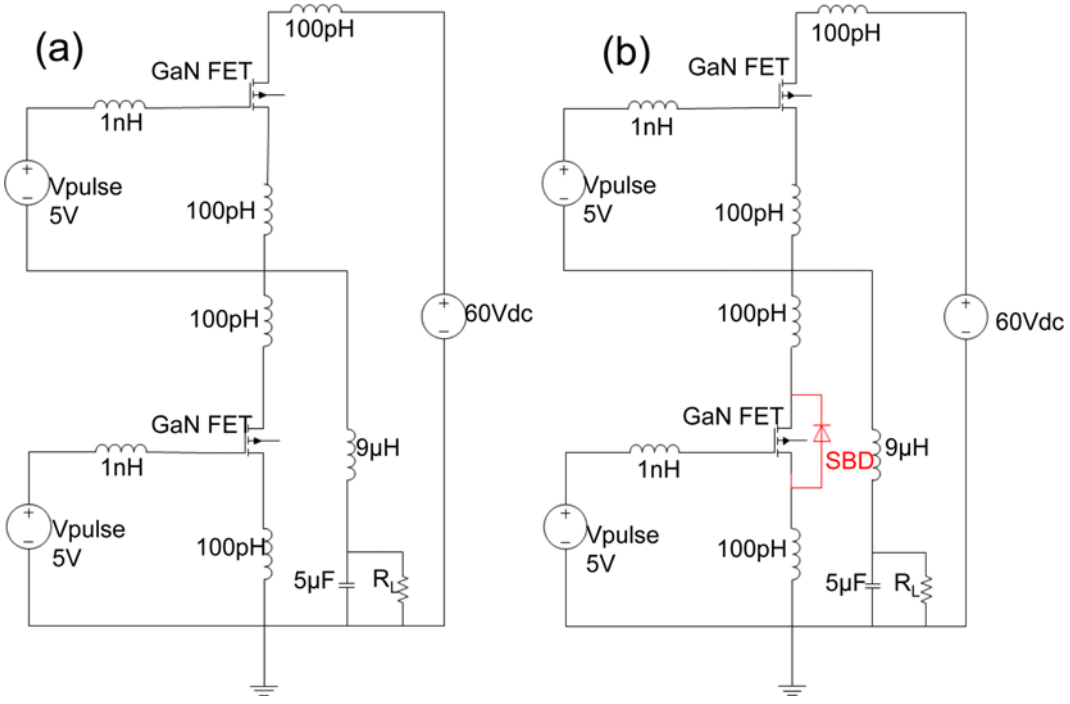

Fig. 1. Synchronous DC-DC 60 V - 10 V converter circuit diagram (a) without a freewheeling diode and (b) with a freewheeling diode.

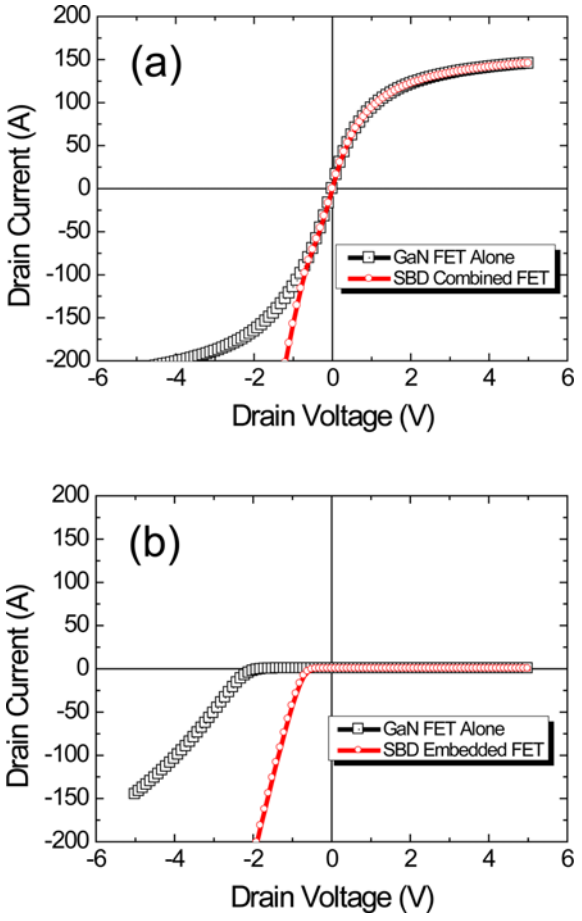

Fig. 2. Comparison of current-voltage characteristics between GaN FET alone and SBD-combined GaN FET. (a) ON state (V_{gs} = 5 V) and (b) OFF state (V_{gs} = 0 V).

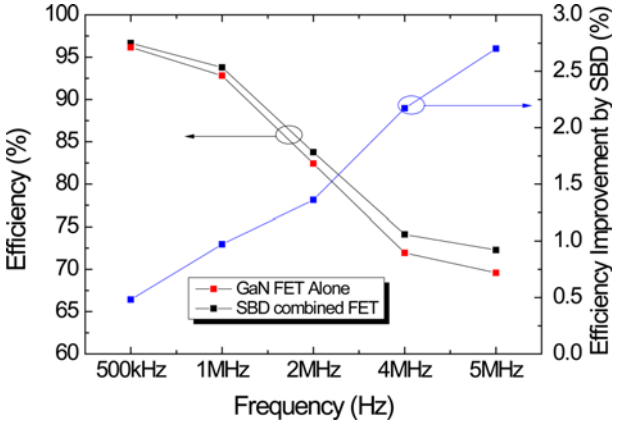

Fig. 3. Simulated conversion efficiency as a function of switching frequency with and without a freewheeling diode. The simulation was carried out for the load current of 2 A.

than 1 MHz. It is obvious that the addition of a freewheeling diode reduces the OFF-state power loss during the dead-time period. The reduction in efficiency at high frequencies is associated with an increased portion of dead-time during

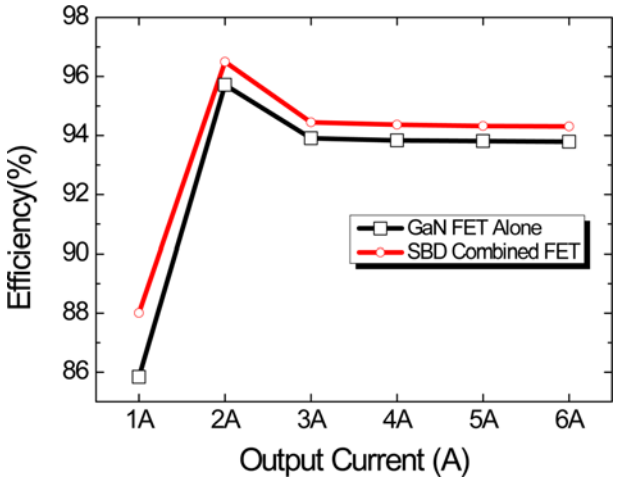

Fig. 4. Simulated conversion efficiency as a function of load current with and without a freewheeling diode. The simulation was carried out at the switching frequency of 1 MHz.

switching operation. Though GaN FETs have a much faster switching capability than Si FETs, the dead-time power loss would limit the ultimate conversion efficiency at high switching frequencies. This limitation becomes worse when GaN FETs have a high threshold voltage because the turn-on voltage of reverse conduction mode is always higher than the forward threshold voltage in conventional GaN FETs. The conversion efficiency characteristics simulated at 1 MHz as a function of the load current are shown in Fig. 4. It should be noted that ~1% improvement in conversion efficiency reflects a significant reduction in loss (e.g., >15% reduction in loss for a 2 A load current in this example). However, adding an extra diode in a circuit increases the overall cost and size of the converter. In order to resolve this trade-off relationship, we propose a novel GaN FET with an embedded freewheeling diode, which is discussed in the following section.

2.2 Freewheeling-Diode-Embedded GaN MOSHFET

In general, a freewheeling diode is externally connected to the switching FET. An alternative way to implement the freewheeling diode would be to monolithically fabricate the diode on a single chip. However, the chip area would be almost doubled by the presence of the additional diode. In this study, we suggest a novel device structure composed of a normally-off GaN FET with an embedded freewheeling SBD. The proposed device structure is shown in Fig. 5 in comparison with a conventional GaN MOSHFET. The normally-off mode transistor is implemented by a recessed MOSHFET configuration, whereas the freewheeling diode is done by an SBD. The remaining AlGaN barrier thickness under the recessed gate region is 3 nm, and the gate oxide (SiO_2) thickness is 30 nm. The recessed gate region makes the 2DEG channel completely depleted with zero gate bias

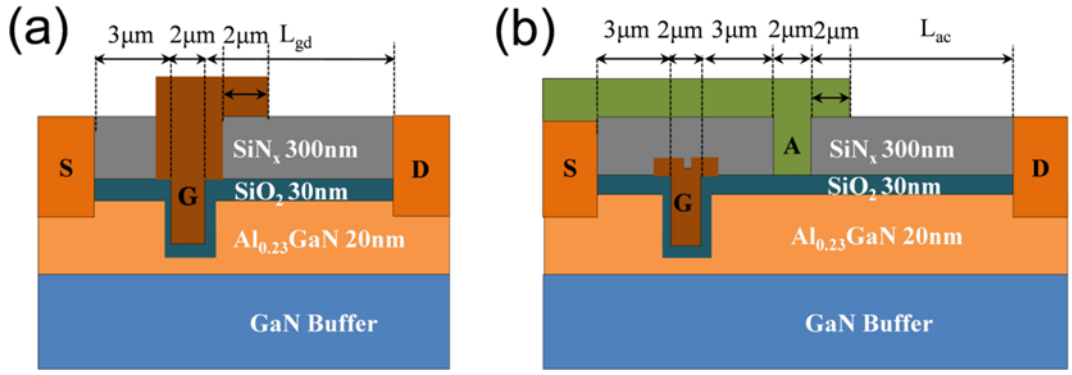

Fig. 5. Cross-sectional schematics of (a) conventional recessed GaN MOSHFET and (b) SBD embedded GaN MOSHFET.

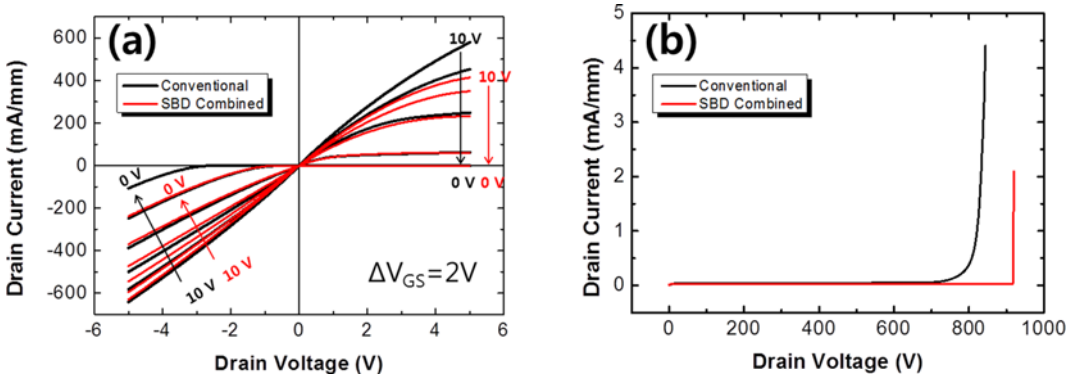

Fig. 6. Comparison of simulated (a) current voltage and (b) breakdown characteristics between conventional and SBD embedded GaN MOSHFETs. Both L_{gd} for the conventional device and L_{ac} for the SBD embedded device were 8 μm.

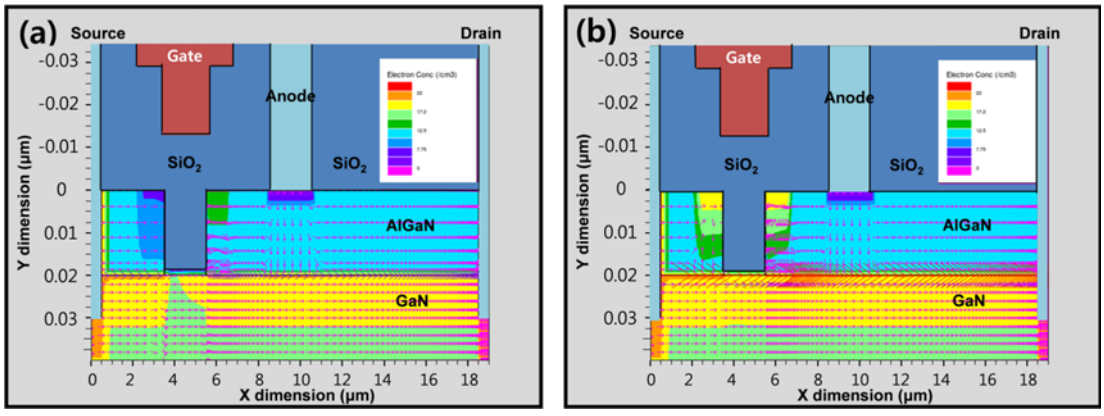

Fig. 7. Current flow phenomena for SBD embedded GaN MOSHFET simulated at (a) V_{ds} = −2 V and V_{gs} = 0 V and (b) V_{ds} = −2 V and V_{gs} = 10 V. The contours indicate the electron density distribution whereas the arrows indicate the current density and direction. The larger arrows mean higher current density.

condition.[12] In the proposed device, the anode electrode of the SBD is located between the gate and drain electrodes and is electrically connected to the source electrode, whereas the drain plays a role as a cathode. The anode length is 2 μm and the distance from the gate to the anode is 3 μm.

The simulated current-voltage and breakdown characteristics for the conventional and proposed devices are compared in Fig. 6, where L_{gd} and L_{ac} are 8 μm for both structures. The operation principle of the proposed device is as follows. During the forward operation with a positive drain bias (see the first quadrant in Fig. 6(a)), the Schottky anode is in reverse bias condition. Thus, no current flows through the anode, whereas the gate controls the current conduction between the drain and the source just as a conventional

Table 1. Comparison of device characteristics between conventional and SBD embedded devices.

L_{GD} or L_{AC} (μm)	On state forward voltage drop @0.1 A/mm (V)		On state reverse voltage drop @0.1 A/mm (V)		Off state reverse voltage drop @0.1 A/mm (V)		Breakdown Voltage (V)	
	Conventional	SBD embedded	Conventional	SBD embedded	Conventional	SBD embedded	Conventional	SBD embedded
8	0.7	0.85	-0.7	-0.8	-5.0	-3.0	840	920

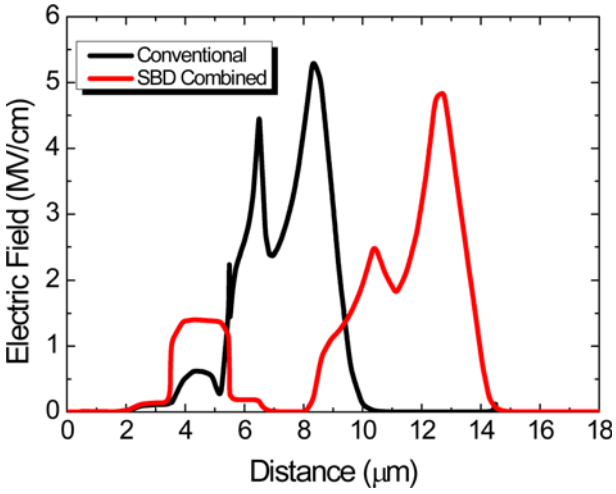

Fig. 8. Comparison of electric field distribution between conventional and SBD embedded devices. Both L_{gd} for the conventional device and L_{ac} for the SBD embedded device were 8 μm. The data were captured at the drain voltage of 800 V with the gate voltage of 0 V.

device. During the reverse operation with a negative drain bias (see the third quadrant in Fig. 6(b)), the Schottky anode is now in forward bias condition, allowing the current flow through the Schottky anode even without turning on the gate (i.e. during the dead-time). The simulated current flow under this condition is shown in Fig. 7(a) in which the drain voltage is −2 V and the gate voltage is 0 V. It is seen that the current flows through the embedded Schottky anode while the gate bias is in OFF state. With the gate bias of the ON state, the FET current is added to the drain current, which is shown in Fig. 7(b) where the drain voltage is −2 V and the gate voltage is 10 V.

The simulated forward and reverse characteristics are summarized in Table 1. Though the forward current density of the proposed device is relatively lower than that of the conventional device, due to the additional space required for the Schottky anode embedment, the breakdown voltage of the proposed device is higher than that of the conventional device. According to the simulated electric field distribution, the peak electric field strength in the proposed device is lower than that in the conventional device, as shown in Fig. 8. The biggest advantage of the proposed device is the superior reverse conduction, with a much lower threshold voltage during the OFF state (zero gate bias), which will reduce the dead-time power loss. It should also be noted that the proposed structure saves significant chip area in comparison with the combination of an individual FET and a diode. It is suggested that the proposed device will be more beneficial for higher breakdown voltage specifications, as the additional space required for Schottky anode embedment becomes insignificant.

3. CONCLUSIONS

The benefits of using a freewheeling diode in a GaN based synchronous buck converter have been investigated. Although the conversion efficiency can be improved by adding a freewheeling SBD, the increase in overall cost and chip size must be taken into account when designing GaN based converters. In order to minimize the cost and size increase, a novel SBD-embedded AlGaN/GaN MOSHFET structure was proposed and its characteristics were investigated based on 2-dimensional device simulation. Since the proposed device eliminates the need for an external diode, the conversion efficiency can be maximized without much increase in production cost.

ACKNOWLEDGEMENTS

This work was supported by Korea Electric Power Corporation Research Institute through Korea Electrical Engineering & Science Research Institute (grant number: R13DA14) and Nano Material Technology Development Program (NRF-2012M3A7B4035274) through National Research Foundation of Korea (NRF) grant funded by the Korean Government.

REFERENCES

1. W. Saito, T. Nitta, Y. Kakiuchi, Y. Saito, I. Omura, and M. Yamaguchi, *IEEE Trans. Electron Devices*, **54**, 1825 (2007).
2. T. Funaki, M. Matsushita, M. Sasagawa, T. Kimoto, and T. Hikihara, *IEEE Applied Power Electronics Conf. Expo.*, p. 339 (2007).
3. M. Farahmand, C. Garetto, E. Bellotti, K. F. Brennan, M. Goano, E. Ghillino, G. Ghione, J. D. Albrecht, and P. P. Ruden, *IEEE Trans. Electron Devices,* **48**, 535 (2001).
4. Y. Uemoto, M. Hikita, H. Ueno, H. Matsuo, H. Ishida, M. Yanagihara, T. Ueda, T. Tanaka, and D. Ueda, *Proc. IEEE International Electron Devices Meeting*, p. 151, IEEE Inst. Elec. Electron. Eng. Inc., Washington D.C., USA (2009).

5. J.-G. Lee, B.-R. Park, H.-J. Lee, M. Lee, K.-S. Seo, and H.-Y. Cha, *Appl. Phys. Express.*, **5**, 066502 (2012).
6. R. Mitova, R. Ghosh, U. Mhaskar, M. Wang, and A. Dentella, *IEEE Trans. Power Electron.*, **29**, 2441 (2014).
7. K.-H. Hong, H.-S. Choi, I.-J. Hwang, and J.-S. Kim, *Electron. Mater. Lett*. **10**, 363 (2014).
8. M. Siva Pratap Reddy, J.-H. Lee, and J.-S. Jang, *Electron. Mater. Lett*. **10**, 411 (2014).
9. T. Morita, S. Ujita, H. Umeda, Y. Kinoshita, S. Tamura, Y. Anda, T. Ueda, and T. Tanaka, *Proc. IEEE International Electron Devices Meeting*, p. 151, IEEE Inst. Elec. Electron. Eng. Inc., San Francisco, USA (2012).
10. Diodes Incorporated, *MBR20100CTP datasheet*, http://www.diodes.com/datasheets/ds31413.pdf (2011).
11. EPC, *eGaN FET EPC2010 datasheet*, http://epc-co.com/epc/documents/datasheets/EPC2010_datasheet.pdf (2013).
12. B.-R. Park, J.-G. Lee, W. Choi, H. Kim, K.-S. Seo, and H.-Y. Cha, *IEEE Electron Device Lett.* **34**, 354 (2013).